Mechanical heterogeneity and mechanism of plasticity in metallic glasses

J. G. Wang,[1] D. Q. Zhao,[1] M. X. Pan,[1] C. H. Shek,[2] and W. H. Wang[1,a)]
[1]*Institue of Physics, Chinese Academy of Sciences, Beijing 100190, People's Republic of China*
[2]*Department of Physics and Materials Science, City University of Hong Kong, Hong Kong, People's Republic of China*

(Received 1 November 2008; accepted 5 January 2009; published online 22 January 2009)

The mechanical heterogeneity is quantified based on the spatial nanohardness distributions in three bulk metallic glasses with different plasticities. It is found that the metallic glass with high mechanical heterogeneity is more plastic. We propose that the appropriate mechanical heterogeneity makes the metallic glasses meliorate their plasticity by increasing inelastic strained area and promoting energy dissipation. © *2009 American Institute of Physics*. [DOI: 10.1063/1.3073985]

Heterogeneities of structure and properties exist in almost all kinds of materials.[1–6] Inclusion, vacancy, defect, and grain boundary usually result in microscale heterogeneity of a material.[1,3–6] Although the heterogeneity defies accurate experimental and theoretical analyses, it plays a key role in physical and mechanical properties of a material.[1–6] The mechanical heterogeneity can promote energy dissipation in bone in nanoscale[4,5] and stabilize Larsen C ice shelf through limiting the propagation of the rift.[6] The structural heterogeneity can affect the strength of cement excelsior board due to the alignment of strands[2] and control the fracture way of ceramics and rocks.[3] However, metallic glass seems to have a different situation.[7,8] There is so far no general agreement on its microscopic structure in spite of great effort. Only homogeneous contrast can be seen even when using the state-of-the-art high resolution transmission electron microscopy (HRTEM). The random closed cluster packing model is proposed for the microstructure of the metallic glass,[9] which is regarded as homogeneous and featureless in nanoscale.

Recently, microscopic heterogeneity has been found in (YTi)-, Ti-, (CuZr)-, Zr-, and Ni-based bulk metallic glasses (BMGs).[10–13] This kind of heterogeneity is generally ascribed to liquid phase separation because there exist two distinguishable contrasts in the TEM image, and the compositions of the two phases are evidently different.[10–13] The phase separation induced heterogeneity can enhance or deteriorate the plasticity of the BMGs, depending on its length scale.[9–14] More recently, an exceptional large compressive plasticity is obtained in ZrCuNiAl BMGs.[15] The microstructure investigation shows a unique structural feature: the dark regions surrounded by bright regions. The different regions are found to have the same composition.[15] The hardness difference between the two regions is regarded as the cause for the large plasticity.[15] However, it is necessary to corroborate the mechanical heterogeneity and elucidate how the heterogeneity affects the mechanical properties of a BMG.

In this letter, we measured the spatial nanohardness distribution of three BMGs with markedly different plasticities, namely, brittle $Fe_{41}Co_7Cr_{15}Mo_{14}C_{15}B_6Y_2$ (Fe-based),[16] $Zr_{64.13}Cu_{15.75}Ni_{10.12}Al_{10}$ (ZrCuNiAl) (Ref. 15) with exceptional plasticity, and intermediate $Zr_{46.75}Ti_{8.25}Cu_{7.5}Ni_{10}Be_{27.5}$ (Vit4) by nanoindentation. The degree of mechanical heterogeneity of the three BMGs is quantified in terms of the distribution of the nanoindentation hardness in microscale, and the origin of the heterogeneity was also studied. The results suggest a rational correlation between the plasticity and the mechanical heterogeneity of the BMGs.

The samples of the three BMGs (Ref. 7) for nanoindentation were cut to $8\times1.5\times1$ mm^3 in size and carefully polished to make the surface smooth. After checking the smoothness of the surface using scanning electron microscope (SEM), the indentations were carried out over a square area of 20×20 μm^2 for Fe-based BMG and Vit4 and 40×40 μm^2 for ZrCuNiAl in a Nano Indenter XP (MTS) with a Berkovich-type tip. All indentations were programed to penetrate the same depth, viz., 150 nm, and the spacing between adjacent indentations was 2 μm. The loading velocity was ~1.3 nm/s. A Philips XL30 SEM and a TECNAI-F20 TEM equipped with EDX were used to examine the samples. The samples for TEM experiments were subjected to ion milling at an incident angle 15° using a Gatan 691 with liquid nitrogen cooling.

Figure 1(a) illustrates the nanoindentation operation on the surface of the sample. The smoothness of the surface was examined by SEM, as shown in Fig. 1(b) for ZrCuNiAl. Similar SEM images of Fe-based BMG and Vit4 are not

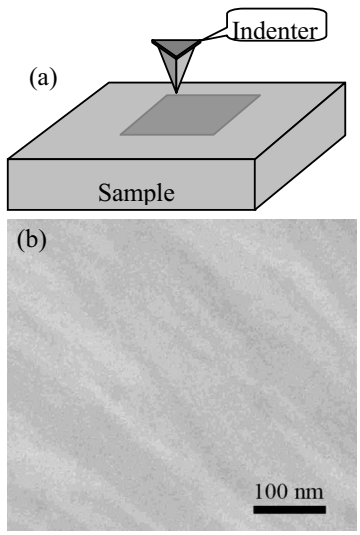

FIG. 1. Schematic diagram of the nanoindentation performance on the polished surface of the sample. (a) Illustration of the indentation on a selected square area (dark gray). (b) The SEM examination of the smoothness of the surface.

a)Author to whom correspondence should be addressed. Electronic mail: whw@aphy.iphy.ac.cn.

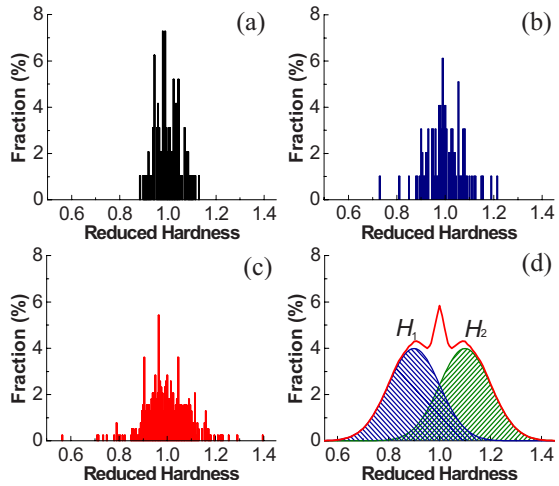

FIG. 2. (Color online) The distributions of the reduced nanoindentation hardness (a) for Fe-based, (b) for Vit4, and (c) for ZrCuNiAl. (d) A sketch is used to illustrate the formation of the three peaks in (c); the highest peak results from the superposition of the two normal distributions with mean value H_1 and H_2.

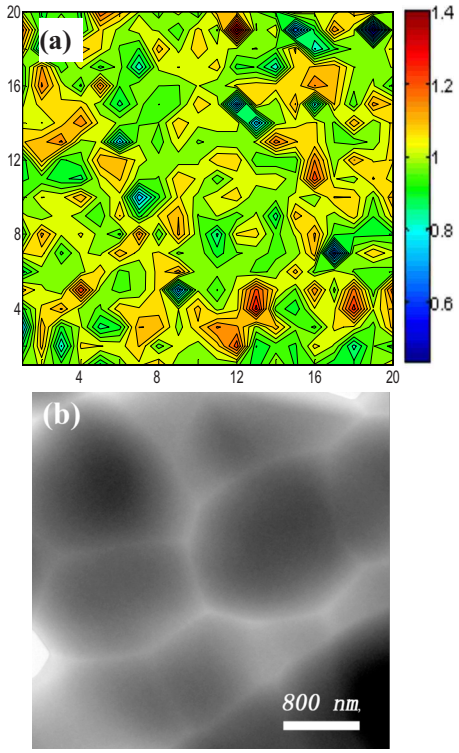

FIG. 3. (Color online) (a) The microstructure of the as-cast ZrCuNiAl in TEM. (b) The contour-line map of the nanoindentation hardness values over a square area on the surface of the ZrCuNiAl shows the microscale mechanical heterogeneity: the hard regions (orange and red) are surrounded by the continuous soft regions (green and blue).

shown here. Only indistinct scratches, which have only trivial influence on the result of nanoindentation, can be found on the sample surface. Given the geometry and dimension of the probe tip, an indentation impression ~800 nm in size is left. Although the shear bands usually develop around the indents, they rarely extend the strain to an outer area as large as the impression itself.[13,17] In other words, the size of the entire strained zone of an indentation is ~1.6 μm in this work. Therefore, the distance of 2 μm between two neighboring indentations was chosen to avoid overlapping of neighboring strained zones. The relative nanohardness is introduced instead of the absolute quantitative value to minimize the effect of scratch. To compare the spatial hardness distributions among the three BMGs, the reduced hardness h_{ri} is determined as $h_{ri}=h_i/H$ ($H=(1/n)\Sigma_i h_i$, h_i is ith nanohardness value). Histograms (a), (b), and (c) in Fig. 2 characterize the nanohardness distribution of Fe-based BMG, Vit4, and ZrCuNiAl, respectively. Clearly, h_{ri} mainly distributes between 0.9 and 1.1 for Fe-based BMG, 0.8 and 1.2 for Vit4, and 0.7 and 1.3 for ZrCuNiAl, which means that the plastic BMG has a wider distribution of hardness than its brittle counterparts. The highest fraction peak value is 7.3 for Fe-based BMG when $h_{ri}=0.99$, 6.1 for Vit4 when $h_{ri}=0.99$, and 5.4 for ZrCuNiAl when $h_{ri}=0.96$, indicating that the nanohardness values of the brittle BMG tend to centralize to the mean value H. Through Jarque–Bera testing, the nanohardness values conform with the normal distribution in Fe-based BMG and Vit4 but inhomogeneous in ZrCuNiAl. This indicates that the brittle BMG, in contrast to the plastic BMG, should have a uniform hardness throughout the whole sample. Moreover, ZrCuNiAl has two secondary fraction peaks of the same value of 3.6 when $h_{ri}=0.90$, 1.05 [see Fig. 2(c)]. The highest peak is supposed to originate from the superposition of the two normal distributions with different mean values of H_1 and H_2, as illustrated in Fig. 2(d). That means the ZrCuNiAl BMG has a dual hardness (soft and hard) in microscale.

The contour map in Fig. 3(a) shows the spatial distribution of reduced hardness values h_{ri} of ZrCuNiAl over a 40 $\times$40 μm^2 square area. One can see that the islands with high h_{ri} values are surrounded by a continuous zone with low h_{ri} values. This map, to some extent, reflects the mechanical configuration of ZrCuNiAl in microscale. Correspondingly, the TEM observation [Fig. 3(b)] shows a typical microstructure of ZrCuNiAl: isolated dark regions are surrounded by continuous bright regions, which cannot be seen in other two BMGs. More importantly, the selected area electron diffraction (SAED) and HRTEM in bright and dark regions demonstrate the glassy nature in both regions.[15] Contrast distinction in TEM bright-field images arises from thickness variation. The bright zones are thinner than the dark ones, and these different thicknesses indicate that the thinning rate in bright zones is higher than in dark zones upon ion milling. The faster thinning in bright zones implies that they are weaker in bonding than dark ones. So we think the TEM images are evidence for the existence of the hard and soft regions. The observation is consistent with that of the fluctuation in nanohardness measured by nanoindentation tests, which indicates that there exists mechanical heterogeneity in ZrCuNiAl BMG.

Ichitsubo *et al.*[18] found that strongly bonded regions are surrounded by weakly bonded regions in $Pd_{40}Ni_{40}P_{20}$ BMG from the ultrasound-accelerated crystallization results. The weakly bonded regions were found thermodynamically less stable than the strongly bonded regions.[18] The crystallization behaviors of the bright and dark regions in ZrCuNiAl should be different in the annealing process. To confirm this assumption, the ZrCuNiAl samples were isothermally annealed at different temperatures around the glass transition temperature T_g ~ 375 °C and then examined by TEM. Figure 4(a) exhibits the microstructure of the sample annealed at 385 °C for 2 h. Compared with that of the as-cast sample [Fig. 3(a)], the bright and dark regions can still be clearly seen. How-

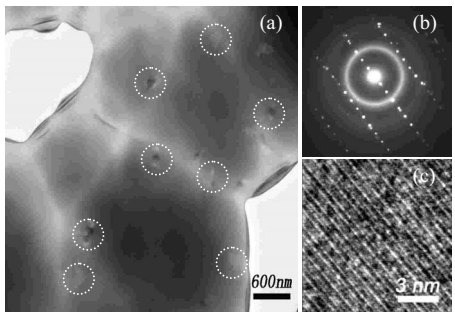

FIG. 4. The thermodynamic stability investigation for the bright and dark regions in the ZrCuNiAl. (a) TEM image from the sample annealed at 385 °C for 2 h shows that only bright regions precipitate nanocrystallites (circled by dashed line) ascertained by (b) SAED and (c) HRTEM.

ever, only in bright regions can one observe the precipitation of nanocrystallites ascertained by SAED [Fig. 4(b)] and HRTEM [Fig. 4(c)]. For the sample annealed at higher temperature of 398 °C for 2 h, the crystalline grains grow distinctly larger, but the dark regions are still in glassy state. This does confirm that the bright regions are thermodynamically less stable compared to that of the dark regions, which indicates that the bright region is softer than the dark region in ZrCuNiAl. In the atomic scale, the bright region should have more free volume than the dark region, so the atoms in the bright region can move or jump much more easily when stressed, which results in the mechanical response difference between the two regions.[19]

The coexistence of soft/ductile and hard/brittle phases had been noticed in crystalline alloys, and the mechanical properties of the alloys depend on how the two phases are distributed.[1] A combination of optimum strength and ductility is achieved when the hard phases are uniformly embedded throughout the soft matrix.[1] In ZrCuNiAl, as shown in Fig. 3, the distribution of the hard and soft regions meets the optimum combination conditions, which is practically verified by its superior mechanical properties.[15] Conversely, a Zr-based BMG consisting of a soft phase and a hard phase resulting from liquid phase separation[12] is much less plastic compared to that of the ZrCuNiAl. According to the microstructure investigation, the soft phase in the Zr-based BMG is separated by the hard phase, whereas the soft region in the ZrCuNiAl forms a continuous and random network throughout the whole sample.[12,15]

The shear transformation zones occur preferentially in soft regions with lower critical shear stress and evolve into shear bands once the BMG yielding loaded. For the ZrCuNiAl, the soft regions of a continuous network enable numerous shear bands to concurrently initiate at different sites to accommodate the applied strain and prevent few primary shear bands from carrying severe strain and inducing the fracture. On the other hand, when a shear or a crack propagates, it will unavoidably interact with the soft region, owing to the connectivity of soft region throughout the whole sample. The stress concentration at the shear front or crack tip, as a result, is mitigated through the viscous/plastic flow of the soft phase. The shear bands are then retarded, rechannelled, or bifurcated. Consequently, a larger volume fraction of shear bands or microcracks formed, which contributes to the plastic deformation. The situation is similar to that in bone where the micromechanical heterogeneity of the structure remarkably improves energy dissipation through increasing the inelastically deformed area twice as large as the homogeneous case.[4] The soft and hard models for explanation of plasticity are also consistent with the explanation of plasticity in terms of a high Poisson ratio v.[20–22] The slight fraction increase in soft regions would augment v steeply and, in turn, markedly enhance the plasticity.[15]

In fact, the mechanical heterogeneity also exists in the BMG-based composites, owing to the elastic modulus variation between the introduced crystalline phase (soft) and the glassy matrix (hard).[23,24] The ductile dendrite phase in the glassy matrix plays a role similar to that of the soft region in ZrCuNiAl. Besides, the ductile phase must account for a critical volume fraction to make itself percolate through the sample, such as the continuity of the soft region in ZrCuNiAl. The superior mechanical properties of the composites indicate that the mechanical heterogeneity is beneficially effective.

In summary, the ZrCuNiAl with a large plasticity has a bimodal hardness distribution resulting from the soft and hard regions, which are experimentally found to possess different thermodynamic stability. The suitable distribution of the soft and hard regions can effectively improve the plasticity of the BMG.

Financial support was from NSF of China (Grant Nos. 50621061 and 50731008) and MOST 973 (Grant No. 2007CB613904).

[1] G. E. Dieter, *Mechanical Metallurgy* (McGraw-Hill, New York, 1988).
[2] D. C. Stahl, S. M. Cramer, and R. L. Geimer, Wood Fiber Sci. **29**, 345 (1997).
[3] K. Bhattacharya and G. Ravuchandran, J. Mech. Phys. Solids **46**, 2171 (1998).
[4] K. S. Tai, M. Dao, S. Suresh, A. Palazoglu, and C. Ortiz, Nature Mater. **6**, 454 (2007).
[5] J. Currey, J. Musc. Neur. Interact **5**, 317 (2005).
[6] B. Kulessa and P. R. Sammonds, Geophys. Res. Abstr. **9**, 03645 (2007).
[7] X. K. Xi, D. Q. Zhao, M. X. Pan, W. H. Wang, Y. Wu, and J. J. Lewandowski, Phys. Rev. Lett. **94**, 125510 (2005).
[8] J. H. Li, X. D. Dai, S. H. Liang, K. P. Tai, Y. Kong, and B. X. Liu, Phys. Rep. **455**, 1 (2008).
[9] D. B. Miracle, Nature Mater. **3**, 697 (2004).
[10] E. S. Park, H. J. Chang, J. Y. Lee, and D. H. Kim, J. Mater. Res. **22**, 3440 (2007).
[11] J. Das, M. B. Tang, K. B. Kim, R. Theissmann, F. Baier, W. H. Wang, and J. Eckert, Phys. Rev. Lett. **94**, 205501 (2005); M. B. Tang, D. Q. Zhao, M. X. Pan, and W. H. Wang, Chin. Phys. Lett. **21**, 901 (2004).
[12] X. H. Du, J. C. Huang, H. M. Chen, and P. K. Liaw, Appl. Phys. Lett. **91**, 131901 (2007).
[13] A. Concustell, N. Mattern, H. Wendrock, U. Kuehn, A. Gebert, J. Eckert, A. L. Greer, J. Sort, and M. D. Baró, Scr. Mater. **56**, 85 (2007).
[14] K. B. Kim, X. F. Zhang, S. Yi, J. Das, and J. Eckert, Philos. Mag. Lett. **88**, 75 (2008).
[15] Y. H. Liu, G. Wang, D. Q. Zhao, and W. H. Wang, Science **315**, 1385 (2007).
[16] Q. J. Chen, J. Shen, D. L. Zhang, H. B. Fan, and J. F. Sun, J. Mater. Res. **22**, 358 (2007).
[17] M. W. Chen, Annu. Rev. Mater. Res. **38**, 445 (2008).
[18] T. Ichitsubo, E. Matsubara, and T. Yamamoto, Phys. Rev. Lett. **95**, 245501 (2005).
[19] F. Spaepen, Acta Metall. **25**, 407 (1977).
[20] J. Schroers and W. L. Johnson, Phys. Rev. Lett. **93**, 255506 (2004).
[21] J. J. Lewandowski, W. H. Wang, and A. L. Greer, Philos. Mag. Lett. **85**, 77 (2005).
[22] X. J. Gu, S. J. Poon, and G. J. Shiflet, Appl. Phys. Lett. **88**, 211905 (2006).
[23] C. C. Hays, C. P. Kim, and W. L. Johnson, Phys. Rev. Lett. **84**, 2901 (2000).
[24] M. L. Lee, Y. Li, and C. A. Schuh, Acta Mater. **52**, 4121 (2004).